



ISSN: 0067-2904

## The Bactericidal Effects of Titanium Nanoparticles on *Staphylococcus aureus* and *Escherichia coli* Utilizing Cold-atmospheric Plasma in Vitro

Zahraa A. Abdul Muhsin<sup>1</sup>, Ghaith H. Jihad<sup>2\*</sup> and Safaa A. Hammed<sup>3</sup>

<sup>1</sup>University of Baghdad, College of Sciences, Department of Biology, Baghdad, Iraq

<sup>2\*</sup>University of Baghdad, College of Sciences, Department of Physics, Baghdad, Iraq

<sup>3</sup>Karkh University of Science, Baghdad, Iraq

Received:11/9/2024

Accepted:6/2/2025

Published: 28/2/2026

### Abstract

The output argon plasma stream was generated, and its properties were studied. The deionized water was formed using the optically described plasma stream. The titanium plate was melted using a needle with the argon gas stream. An analysis was conducted on the emission spectra of the plasma generated within the argon gas plasma jet system at different operating voltages, a flow rate of 4 L/min, and the pressure of the atmosphere. The amounts of NO<sub>2</sub>, NO<sub>3</sub>, and H<sub>2</sub>O<sub>2</sub> that the lab will treat to evaluate their impact on removing bacterial aggregation were determined by measuring the absorbance of the plasma-treated water at wavelengths between 300 and 400 nm. Using optical emission spectrometry (OES), we measured the electron temperature, Debye length, and Debye range while examining the excited titanium metal's spectral lines. A series of spectra generated by the plasma were recorded under different flow rates of argon gas. The temperature and electron band density (T<sub>e</sub>) and (n<sub>e</sub>) of titanium metal and argon gas increased with increasing the flow rate of argon gas into the DC plasma, and increased killing of bacteria was observed with increasing the potential difference of ionized water in the plasma. This study shows that prepared cold plasma has beneficial effects on killing bacteria.

**Keywords :** Cold plasma, activated water, Surface treatment, Argon gas (Ar), Ti-metal.

### التأثيرات القاتلة لجزيئات التيتانيوم النانوية على بكتيريا *S. aureus* و *E. coli* باستخدام بلازما الغلاف الجوي البارد في المختبر

زهراء علي عبدالمحسن<sup>1</sup>, غيث هادي جهاد<sup>2\*</sup>, صفاء علي حميد<sup>3</sup>

<sup>1</sup>قسم علوم الحياة، كلية العلوم، جامعة بغداد، بغداد، العراق

<sup>2</sup>قسم علوم الفيزياء، كلية العلوم، جامعة بغداد، بغداد، العراق

<sup>3</sup>جامعة الكرخ للعلوم، بغداد، العراق

### الخلاصة

تم توليد تيار البلازما الناتج من الأرجون وتمت دراسة خصائصه. تم تشكيل الماء منزوع الأيونات باستخدام تيار البلازما الموصوف بصرياً. باستخدام تيار غاز الأرجون، قمنا بإذابة لوحة التيتانيوم باستخدام إبرة. تم إجراء تحليل على أطيايف الانبعاث للبلازما المتولدة داخل نظام نفث بلازما غاز الأرجون عند جهد تشغيل مختلف ومعدل تدفق 4 لتر / دقيقة وضغط الغلاف الجوي. تم تحديد كميات NO<sub>2</sub> و NO<sub>3</sub> و H<sub>2</sub>O<sub>2</sub>

\*Email: [ghaith.jihad1104@sc.uobaghdad.edu.iq](mailto:ghaith.jihad1104@sc.uobaghdad.edu.iq)

التي سيعالجها المختبر لتقييم تأثيرها على إزالة التجمع البكتيري عن طريق قياس امتصاص الماء المعالج بالبلازما عند أطوال موجية تتراوح بين 300 و 400 نانومتر. باستخدام مطيافية الانبعاث الضوئي (OES) ، قمنا بقياس درجة حرارة الإلكترون وطول ديبراي ونطاق ديبراي أثناء فحص الخطوط الطيفية للمعدن التيتانيوم المثار. تم تسجيل سلسلة من الأطياف الناتجة عن البلازما تحت معدلات تدفق مختلفة لغاز الأرجون. ارتفعت درجة الحرارة وكثافة النطاق الإلكتروني ( $T_e$ ) و ( $n_e$ ) للمعدن التيتانيوم وغاز الأرجون مع زيادة معدل تدفق غاز الأرجون إلى بلازما التيار المستمر، كما لوحظت زيادة في قتل التجمعات البكتيرية مع زيادة فرق الجهد للماء المؤين في البلازما. تظهر دراستنا أن البلازما الباردة المحضرة لها تأثيرات مفيدة في قتل التجمعات البكتيرية.

## 1-Introduction

There is a growing need to study the characteristics of gas-discharge processes to assess their suitability for sterilizing and disinfecting industrial materials, equipment, and electronics. This is done to safeguard them against biological harm and corrosion caused by microorganisms [1,2]. Plasma treatment has been discovered to possess a therapeutic impact on living tissues through the processes of sterilization, hemostasis, and the treatment of skin ailments [3,4]. In recent years, there has been a significant increase in the need for sterilization and disinfection technologies that are efficient, user-friendly, do not require high temperatures, and are very reliable. This trend has gained considerable momentum. The investigation into the characteristics of emissions that produce low-temperature (cold) non-equilibrium plasmas at atmospheric pressure is significant in plasma technologies [11-5] Various gas discharges, such as creeping discharge, corona, barrier, and pulsed discharges, can function as reservoirs of low-temperature, non-equilibrium plasma for chemical reactions, which can be generated under atmospheric pressure. Although many papers have examined different aspects of these discharges and their demonstrated efficacy for biomedical applications in a controlled laboratory setting, the utilization of cold plasma at atmospheric pressure to deactivate microbes has not been widely adopted. The reason behind this is that the plasma sources needed are technically intricate and economically inefficient. Moreover, the utilization of atmospheric pressure discharges to treat biological items necessitates the application of high voltages ranging from 10 to 40 kV, hence presenting a significant safety hazard. Hence, a primary concern in plasma medicine is the selection of discharge settings that provide both safe and nondestructive treatment. The majority of plasma jets typically exhibit a diameter ranging from a few millimeters. Plasma jets with huge diameters and good homogeneity can be generated using a low-current spark discharge in argon at atmospheric pressure. Plasma jets show potential in various applications, including treating large wounds in the medical area. [11]

This investigation involved subjecting two distinct microbial species to cold atmospheric-pressure plasma jets to assess their effectiveness in deactivating the microorganisms. Gram-positive bacteria possess a robust cell wall composed of many layers of peptidoglycan, and Gram-negative bacteria possess an outer membrane. In contrast, gram-negative bacteria possess a stratified composition including three primary components: the outside membrane, the peptidoglycan cell wall, and the inner membrane. The outer membrane serves as an additional stabilizing barrier surrounding the cell, safeguarding it from harmful substances [11].

In this paper, the effect of cold plasma on *S. aureus* and *E. coli* were investigated via the performance of cold plasma at different times of treatment. In addition, the emission spectrum of a plasma jet obtained using a multichannel spectrometer was also analyzed

## 2-Experimental Setup

### 2.1. Plasma jet Generator

In this study, a cold plasma generator is employed. Figure 1 depicts the schematic diagram of the equipment utilized [12]. The device's essential parts include a power supply, a high-voltage converter, a control circuit unit, a plasma-generating circuit, and an air pump. The device also features a discharge chamber, which is essential for producing plasma. The chamber is constructed with air tubing, a metal deflector, an insulated enclosure, positive and negative poles, and a barrier medium. During this experiment, we optimized the device's settings to function at a frequency of 60 Hz. The input voltage was adjusted to around 220 V, while the circuit current utilized was  $2.5 \pm 0.2$ . We calibrated the air pump to get a flow rate of 4 liters per minute. The StarLine AvaSpec-ULS4096CL-EVO fiber optic spectrometer, produced by Avantes in Apeldoorn, The Netherlands, was utilized to analyze the optical emission spectrum (OES) of the cold plasma in the range of (300-900) nm wavelength. To determine the species that were present, we utilized this spectrometer. In addition, we monitored and documented the cold plasma generator's electrical usage, voltage, and individual high-voltage output pulses (plasma doses) for 15 minutes [13]. Additionally, an investigation was carried out to assess the water's electrical conductivity and oxidation-reduction potential (ORP). Treated with cold plasma for each treatment [14].

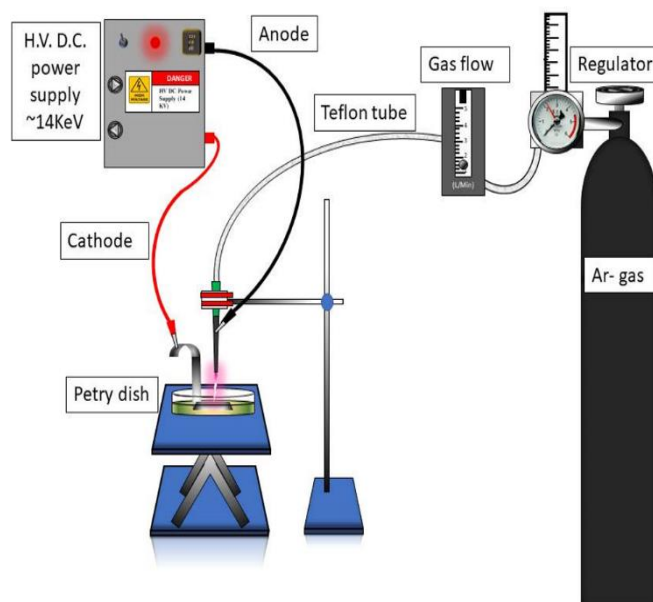


**Figure 1:** Plasma jet experimentation framework diagram

### 2.2. Cell Survivability

The Luria-Bertani (LB) broth was employed for the cultivation of *S. aureus* and *E. coli* until they attained the logarithmic growth phase, which normally required a duration of 2 to 3 hours. Following this, a total volume of 150  $\mu\text{L}$  of the suspensions was spread onto a 90 mm Petri plate containing LB agar culture medium in preparation for plasma treatment and subsequent analysis. Subsequently, the suspensions were diluted to achieve a concentration of  $10^{10}$  colony forming units (CFU) per milliliter (ml) prepared to culture the bacteria for exposure to plasma jetting.

Following the treatment, the Petri dishes were hermetically sealed and incubated for 18-21 hours at  $37^\circ\text{C}$  for *S. aureus* and  $37^\circ\text{C}$  for *E. coli*. Subsequently, the quantity of colony-forming units (CFUs) was enumerated on the Petri dish. The rate of bacterial inactivation was determined by calculating the percentage reduction in CFU numbers of the plasma-treated

sample through the use of software colony count under room temperature. The control sample by dilution is shown in the figures (9) and (10) which are considered before exposing it to plasma jetting at different voltages, and the cause of bacterial killing is due to changing the plasma generation voltage in order to stabilize other factors that are not related to killing. Pathogenic bacteria were obtained from Biology Department, College of Science, University of Baghdad, these bacteria were previously identified by traditional methods, biochemical testing, and then the Vitek method.

### 2.3. Plasma treatment

Figure (2a) displays a diagram illustrating the treatment arrangement. The treating distance is the distance between the PMJ device's exit nozzle and the Petri dish's surface. In this investigation, three voltages (400, 700, and 1000 V) was used to specifically target titanium, at a fixed distance of 1.5 cm for 1 min. The plasma treatment was confined to a square area measuring 2 cm×2 cm in the middle of the Petri dish, which is referred to as the "treated area" (Figure (2b)). The Petri dish containing each bacteria sample was subjected to the plasma torch. The torch moved over the dish at a consistent gas flow speed of 4 L/min. The movement of the torch followed the gridlines as shown in Figure (2b), the torch's movement followed the gridlines. For both *S. aureus* and *E. coli*, the treatment duration was 30 seconds, and the total time for treating each sample ranged from 30 seconds to 1 minute. The experiment was replicated a minimum of three times to determine the average rate of inactivation and measure the variation. We solely exposed the control group to a consistent gas flow rate.

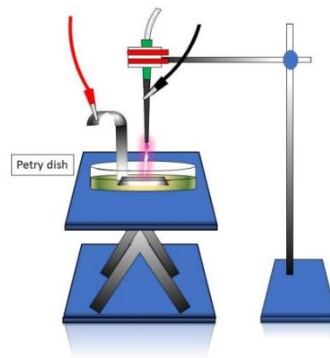


**Figure 2:** Schematic diagram of the PMJ treatment of a Petri dish.

### 2.4 Statistical analysis

The results presented in this study were presented as means derived from the data collected in a minimum of three separate studies, each performed in triplicate, using Origin Lab 2022 for Windows 10. The calculation (decrease in colony forming units/ml) is referred to the untreated (non-plasma) controls compared to plasma treatment. Figure 11, which represents the bacterial colonies of both species before and after treatment and the log<sub>10</sub> reduction in numbers compared to the corresponding untreated (non-plasma) controls, in which the calculation process was done by dividing the sample into four quarters, and using the colony method application, the number of colonies in it was calculated, are shown. A decrease of at least three log<sub>10</sub> orders of magnitude is indicated by Figure 11[15].

## 3-Results and Discussion

### 3.1 Absorption of activated water

When subjected to an atmospheric pressure plasma jet, water undergoes interactions with a range of reactive oxygen and nitrogen species (RONS) that are generated as a result of the plasma emission. The concentration and type of these species can vary based on the plasma generation method and the gas used in the plasma jet, leading to significant changes in the

water's oxidation-reduction potential (ORP), pH, and conductivity compared to untreated water. A volume of ten milliliters of distilled water, which was pure and had its temperature and acidity assessed, was subjected to the plasma jet for one hour to produce the plasma-activated water (PAW). Following the completion of the water treatment process, the levels of H<sub>2</sub>O<sub>2</sub>, NO<sub>3</sub>, and NO<sub>2</sub> were assessed using test strips (Bartovation, USA), as indicated in Table 1. The pH was determined using a pH meter (PH-009(1), China), while the temperature was obtained using a remote infrared thermometer.

**Table 1:** The concentrations of H<sub>2</sub>O<sub>2</sub>, NO<sub>3</sub>, and NO<sub>2</sub>.

Chemical component	Concentration (ppm)
NO <sub>2</sub>	12
NO <sub>3</sub>	110
H <sub>2</sub> O <sub>2</sub>	200
PH	3.5
Temperature before effect	20°C
Temperature after effect	40°C

### 3.2 Plasma parameter diagnosis

#### 3.2.1 Spectroscopy of Optical Emission

Figures (3-5) Display the spectrum of nitrogen gas observed during the diagnosis of plasma jet systems created by argon gas. These figures display many peaks of nitrogen gas within the wavelength range of 300 to 450 nm. The image illustrates the presence of the OH peak at a wavelength of 308 nm, which was further corroborated by the test strips, as indicated in Table (2). The peak with the greatest intensity in the spectrum was observed at a wavelength of 357.69 nm at V=400v, accompanied by smaller peaks on either side [16]. The initial technique employed for sterilizing the utilization of a plasma jet. The gas flow rate was continuously maintained at a fixed rate of 1-4 liters per minute.

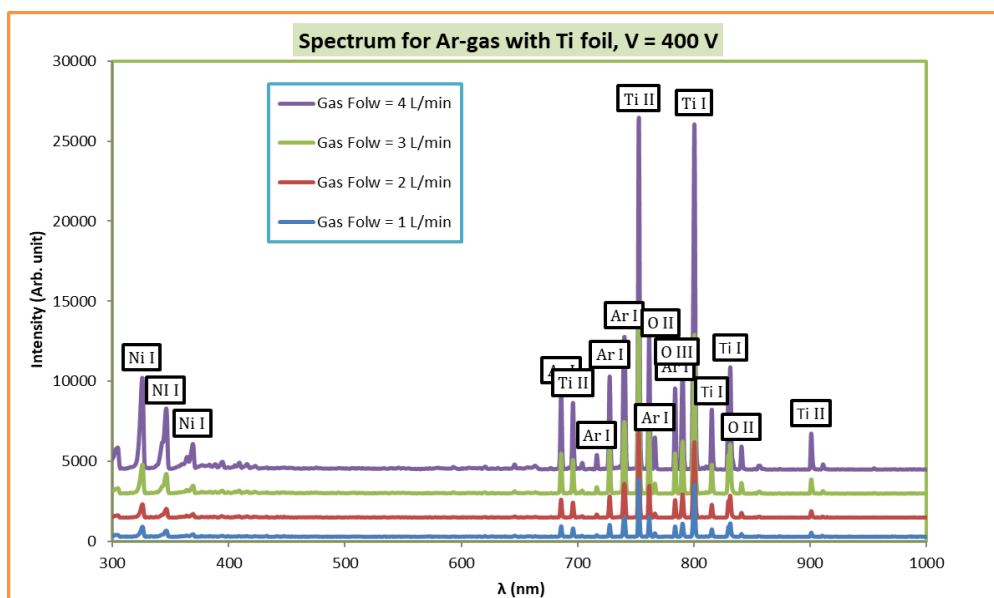


**Figure 3:** The emission spectrum of Ti-foil with V=400V at different gas flows.

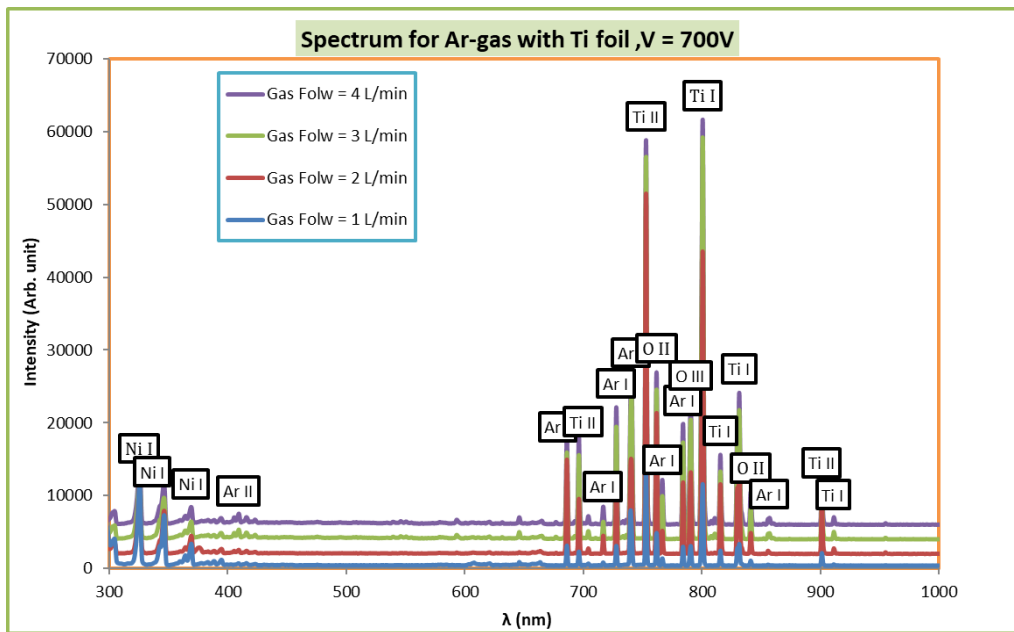


Figure 4: The emission spectrum of Ti-foil with V=700V at different gas flows.

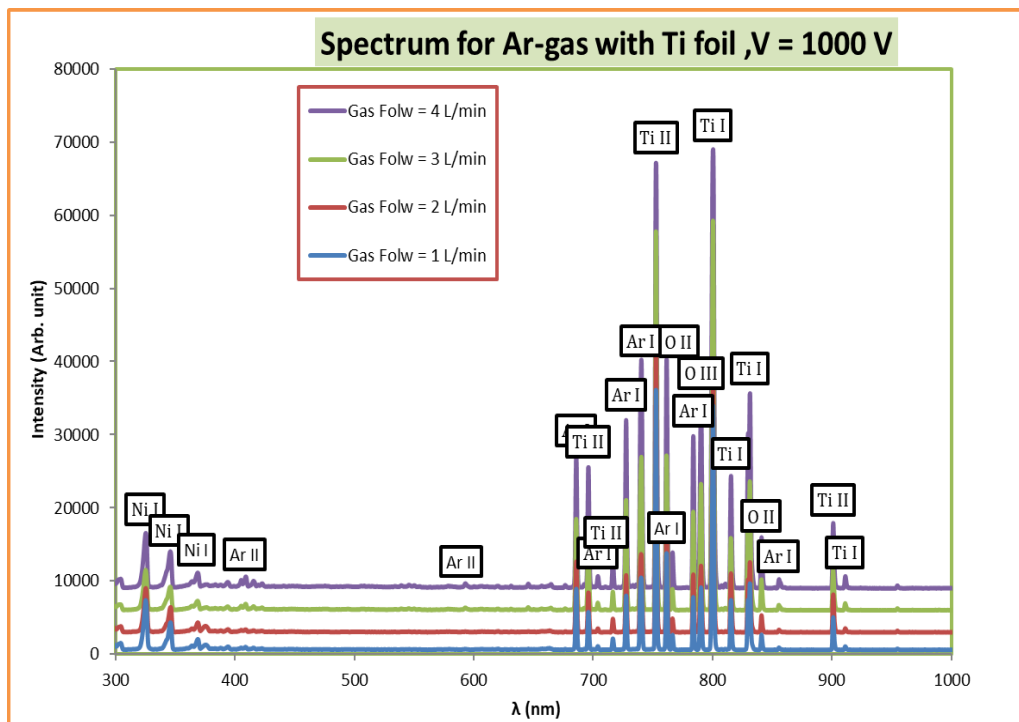


Figure 5: The emission spectrum of Ti-foil with V=1000V at different gas flows.

In the emission spectrum, spectral bands in the 300–400 nm and 700–900 nm wavelength ranges were found. The emissions generated by the second positive system of nitrogen molecules ( $N_2$ ) are observed within the spectral region of 300–400 nm; within this range, strong molecular bands can be identified, which are crucial for understanding various plasma and atmospheric phenomena[17]. Given that  $N_2$  molecules originate from the atmosphere, it may be inferred that the outer section of the plasma jet emitted from the quartz tube contains excited  $N_2$  molecules. The emission observed in the plasma jet is attributed to the excited Ar atoms and Ti molecules. This emission occurs within the spectral range of 700 to 900 nm [18,19]. The findings indicate the existence of electroneutral excited entities within and in the vicinity of the plasma jet, such as excited argon atoms and excited nitrogen molecules.

The plasma jet's emission spectra show that excited N<sub>2</sub> molecules have a peak emission intensity at 335 nm, whereas excited Ar atoms have a peak emission intensity at 761 nm. Hence, the energy levels of the N<sub>2</sub> molecules in an excited state and the Ar atoms in an excited state are 85.5 and 37.6 kcal per mole, respectively. The C-C and C-O bonds possess binding energies valued at 83 and 84 kcal/mol, respectively [20]. When the excited N<sub>2</sub> molecules hit the cell wall and membrane of *E. coli* and *S. aureus* "heightened energy levels result in the breaking of C-C and C-O bonds" This leads to the disruption of the cells. Therefore, these bonds remain intact even when the energized argon atoms come into contact with the cell wall and membrane of *E. coli*, without causing any disruption. Ultimately, the presence of electroneutral excited N<sub>2</sub> molecules could potentially lead to the demise of *E. coli* bacteria.

Ultraviolet radiation with wavelengths between 260 and 280 nm causes harm to the DNA in cells and can eliminate bacteria [20,21]. While examining our emission spectrum, we detected peaks at wavelengths ranging from 260 to 280 nm. However, these peaks exhibited relatively modest intensities [22]. Hence, we hypothesize that the UV light emitted by the plasma jet did not cause any damage or disruption to the cell wall and membrane of the *E. coli*.

The OH radicals produced when electrons in the plasma jet react with H<sub>2</sub>O molecules in the air are responsible for the observed emission in the spectrum. The source of hydroxyl (OH) radicals in a plasma jet primarily stems from the interaction of the plasma with water vapor and liquid water present in the environment. Therefore, we anticipate the presence of OH radicals at the outer edge of the quartz tube's plasma jet. They have a redox potential of 2.85 V, indicating their high oxidative power [23,24].

### 3.2.2 Calculation of electron temperature

The electron temperature ( $T_e$ ) was determined by applying Equation (1) to the line strength ratio, as seen in Figures 6-8. The advantageous benefits of several obstacles were derived from the National Institute of Standards and Technology (NIST) data set utilizing spectra from the Optical emission spectroscopy (OES). The electron densities were computed concurrently with the observed electron temperature.

The line graph depicted in the Figures demonstrates the dependence of the electron's temperature ( $T_e$ ) and density ( $n_e$ ) on the manipulation of the gas flow rate [25]. As the gas flow rate increases, the density of neutral gas molecules also rises. This higher density facilitates more frequent collisions between electrons and neutral particles, which can lead to increased ionization. The greater number of collisions enhances the overall ionization rate, resulting in a higher concentration of free electrons in the plasma. It can be observed that the  $T_e$  and  $n_e$  values in the cold plasma system exhibit an upward trend with an increase in flow rate. Assuming a flow rate of 1 L/min, the electron temperature is 1.295 eV, and the electron density is  $5.12 \times 10^{18} \text{ cm}^{-3}$ . Furthermore, when the flow rate is elevated to 4 liters per minute (L/min), the electron temperature increases to 1.327 eV, and the electron density increases to  $6.10 \times 10^{18} \text{ cm}^{-3}$ .

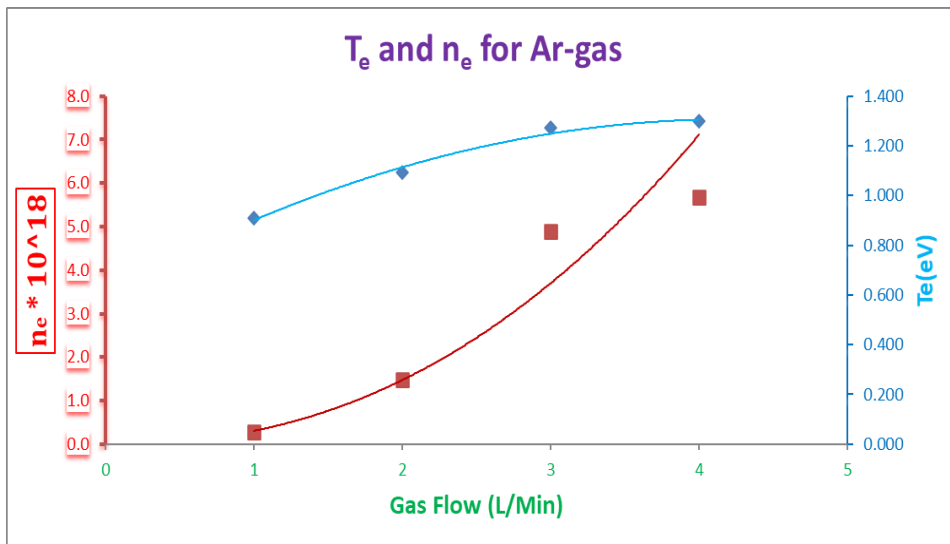


Figure 6: Measurement of  $n_e$  and  $T_e$  of Ti-foil with V=400V at different gas flows.

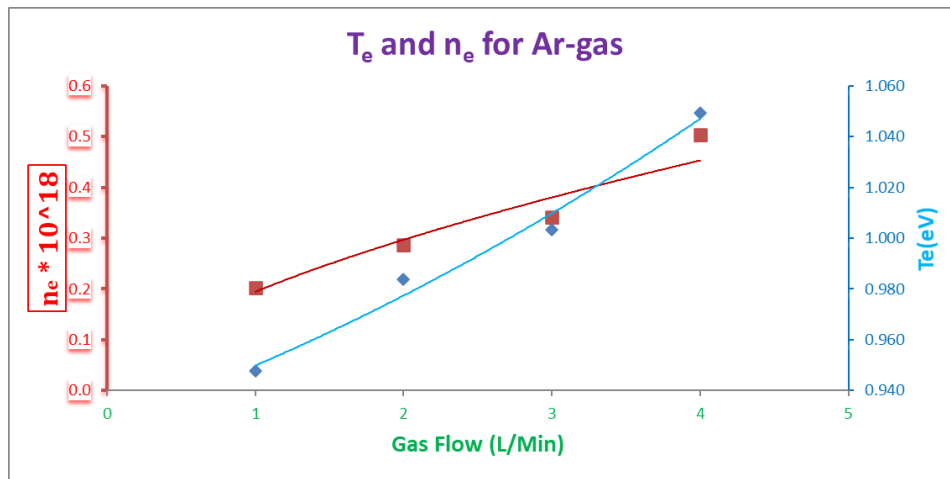


Figure 7: Measurement of  $n_e$  and  $T_e$  of Ti-foil with V=700V at different gas flows.

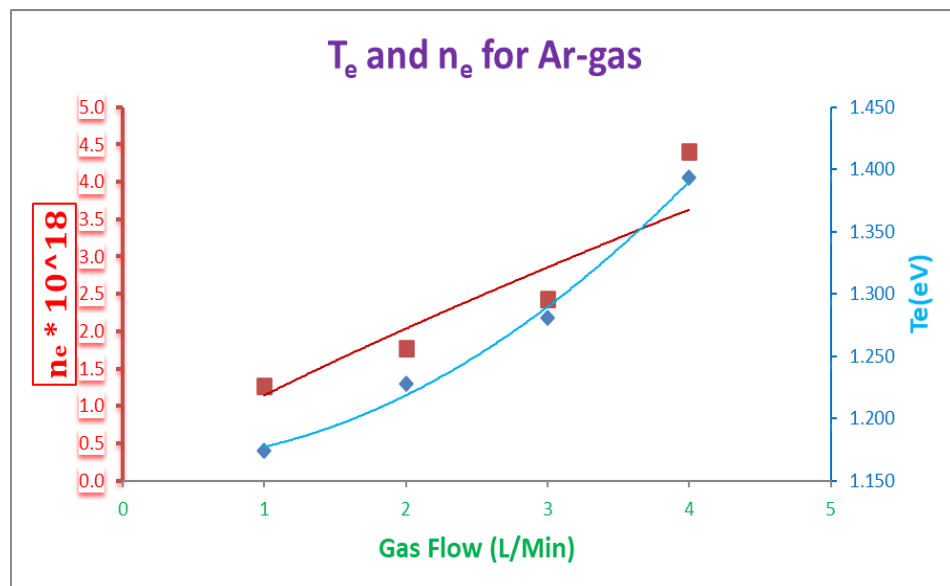


Figure 8: Measurement of  $n_e$  and  $T_e$  of Ti-foil with V=1000V at different gas flows.

The plasma parameters for argon gas are listed in Tables 2-4. Electron density ( $n_e$ ), electron temperature ( $T_e$ ), plasma frequency ( $f_p$ ), Debye length ( $\lambda_D$ ), and Debye number were determined for Ar gas at various flow rates ( $N_D$ ). Plasma parameters estimated ( $\lambda_D$ ,  $f_p$ , and  $N_D$ ) fulfilled the plasma criteria. Since  $f_p$  is proportional to  $m_e$ , it shows that  $f_p$  declines as laser energy increases, but  $f_p$  and  $N_D$  have the opposite (decreasing) trend. This agrees with the results of an earlier study [26].

**Table 2:** Measurements of Plasma Parameters for Ar-gas at V= 400V

Gas Flow (L/Min)	$T_e$ (eV)	$n_e$ (cm <sup>-3</sup> )	$f_p$ (Hz)	$\lambda_D$ (cm)	$N_d$
4	1.358	7.90E+18	2.5E+13	2.9E-05	7.7E+05
3	1.328	6.77E+18	2.3E+13	3.1E-05	8.1E+05
2	1.132	2.03E+18	1.3E+13	5.2E-05	1.2E+06
1	0.935	3.81E+17	5.5E+12	1.1E-04	2.0E+06

**Table 3:** Measurements of Plasma Parameters for Ar-gas at V= 700V

Gas Flow (L/Min)	$T_e$ (eV)	$n_e$ (cm <sup>-3</sup> )	$f_p$ (Hz)	$\lambda_D$ (cm)	$N_d$
4	1.049	5.03E+17	6.4E+12	1.0E-04	2.1E+06
3	1.003	3.41E+17	5.2E+12	1.2E-04	2.4E+06
2	0.984	2.86E+17	4.8E+12	1.3E-04	2.5E+06
1	0.948	2.03E+17	4.0E+12	1.5E-04	2.8E+06

**Table 4:** Measurements of Plasma Parameters for Ar-gas at V= 1000V

Gas Flow (L/Min)	$T_e$ (eV)	$n_e$ (cm <sup>-3</sup> )	$f_p$ (Hz)	$\lambda_D$ (cm)	$N_d$
4	1.393	4.41E+18	1.9E+13	3.9E-05	1.1E+06
3	1.281	2.43E+18	1.4E+13	5.0E-05	1.3E+06
2	1.228	1.78E+18	1.2E+13	5.7E-05	1.4E+06
1	1.174	1.26E+18	1.0E+13	6.7E-05	1.6E+06

### 3.3 Electronic camera imaging

Twenty mL of bacterial suspensions were collected before and after treatment at various voltages. The liquid portion was removed, and the remaining thin layer was subjected to plasma treatment in the treated group, whereas the control group was treated with Argon gas. The sample Ti has a higher level of efficiency, as illustrated in Figures 9 and 10.

The discharge used to treat *E. coli* and *S. aureus* suspended in water solutions with varying electrolytic conductivity levels was a Plasma jet. Figures 9 and 10 display the results of measuring and expressing the bactericidal efficiency as a logarithmic decline. Both *E. Coli* and *S. aureus* showed a larger bactericidal effect; the PMJ system's efficiency was marginally better with high voltage. The reason for this might be the electrospray effect, which involves

spraying the solution of treated water into tiny, measured droplets. This increases the surface-to-volume ratio and makes it easier for reactive oxygen and nitrogen species (RONS) to mass transfer from the gas phase into the solution. The altered RONS chemistry was connected to the greater efficiency found in non-buffered solutions. Table 5 displays the expected efficacy of using the discharge system before and after treatment[27].

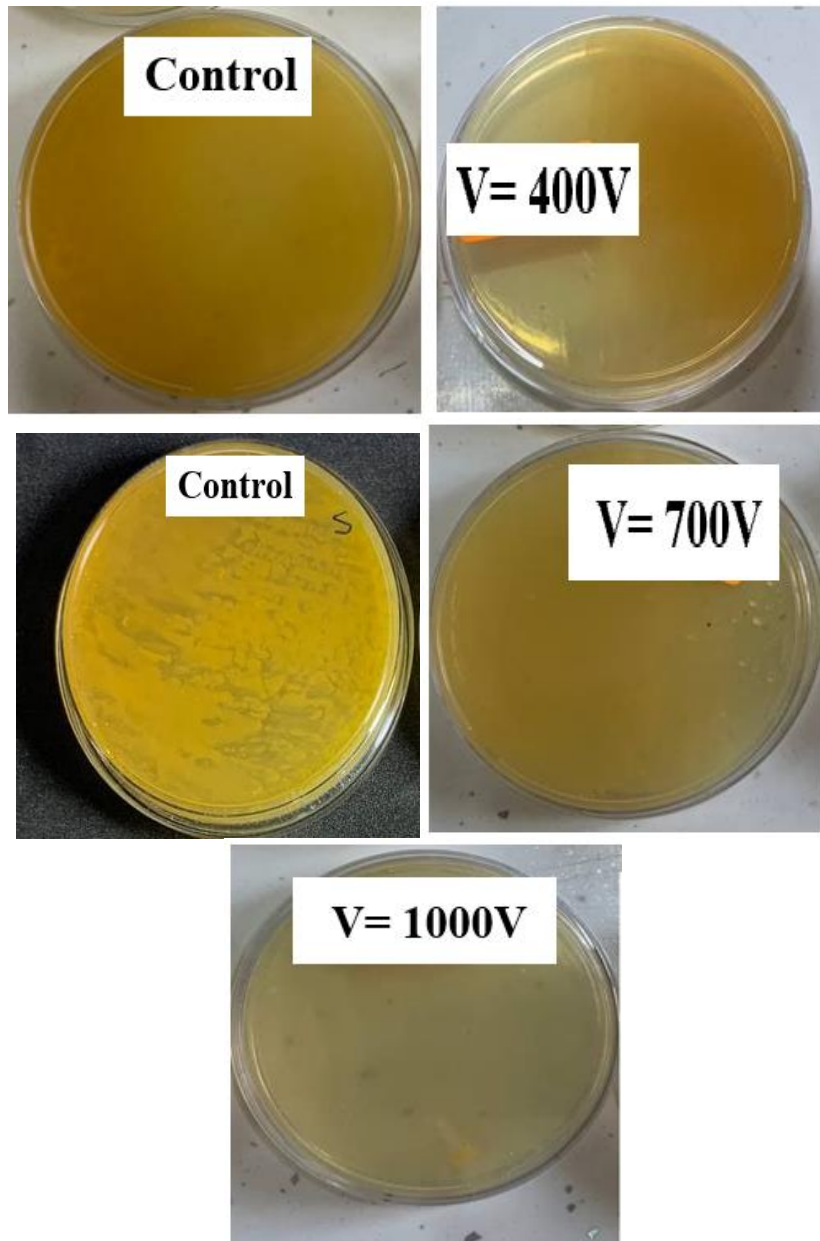


**Figure 9:** Displays images of *E. coli* before (control) and after plasma treatment with Ti metal at various voltages.

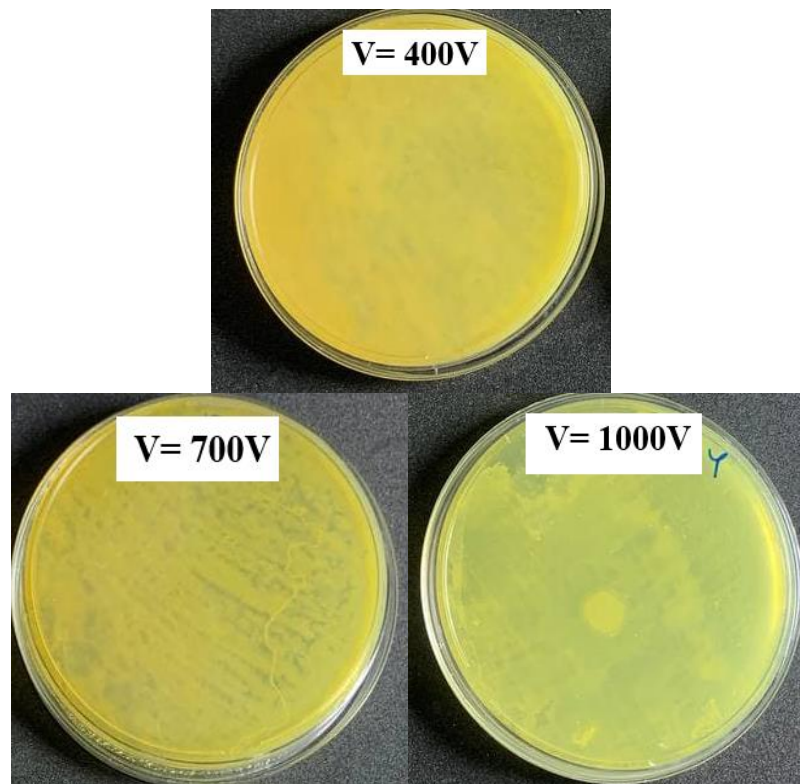


**Figure 10:** Displays images of *S. aureus* before (control) and after plasma treatment with Ti metal at various voltages.

Figures 9 and 10 depict the correlation between the rate of eradication of *E. coli* and *S. aureus* bacteria and various voltages. The initial concentration of *E. coli* colonies before plasma exposure was  $5 \times 10^9$  CFU/ml. The voltage levels of 400, 700, and 1000 V resulted in the killing of *E. coli* bacteria at proportions of  $4.73 \times 10^9$ ,  $1.3 \times 10^9$ , and  $6.1 \times 10^7$  CFU/ml, respectively. During the time that the voltage of 400, 700, and 1000 V resulted in the killing of *S. aureus* bacteria at a proportion of  $4.53 \times 10^9$ ,  $2.4 \times 10^8$ , and  $3.4 \times 10^6$  CFU/ml, respectively. It has been observed that raising the voltage of plasma exposure is a crucial aspect in augmenting the rate of lethality. The bacteria were significantly impacted, resulting in complete eradication when exposed to a high concentration of voltage. The colonies' act of killing is a result of the production of reactive species. The oxygen generated through the contact of plasma with air is crucial for cleansing the afflicted root canals. It achieves this by disturbing the cells and inducing their disintegration through oxidative stress. This work utilized a unipolar plasma jet to treat *E. coli* and *S. aureus* bacteria. The plasma temperature was maintained at  $37^\circ\text{C}$  to ensure that it did not cause any detrimental effects on the live membranes. These methods ensure that the plasma remains safe for use with living tissues by preventing thermal damage while allowing for effective application in biomedical fields such as wound healing, sterilization, and tissue engineering. The results demonstrated that plasma treatment efficiently decreases the colony-forming units (CFU) in the afflicted bacteria, hence enhancing the efficacy of the treatment. The use of voltage enhanced the efficacy of bacterial purification by facilitating the rapid diffusion of free radicals created by the plasma. These radicals immediately interact with subcellular organelles and biomolecules, thanks to the bacteria's robust physical and chemical membrane. The plasma and reactive species' atoms and ions can directly engage with the bacteria. The gradual build-up of charges on the cell membrane leads to its rupture as a result of the coulomb force. Certain reactive species have a prolonged lifespan and undergo breakdown upon contact with the water present on the surface of the tooth. This process results in the formation of potent oxygen compounds[27].

**Table 5:** The results of the number of *E. coli* and *S. aureus* after treatment with different voltages.

Bacterial Type	Voltage			Average	SD
	400	700	1000		
<i>E. coli</i>	4.73 * 10 <sup>9</sup> c	1.3 * 10 <sup>9</sup> b	6.1 * 10 <sup>7</sup> a	2.04 * 10 <sup>9</sup> a	2.4 * 10 <sup>9</sup>
<i>S. aureus</i>	4.53 * 10 <sup>9</sup> c	2.4 * 10 <sup>9</sup> a	3.4 * 10 <sup>7</sup> a	1.59 * 10 <sup>9</sup> b	2.5 * 10 <sup>9</sup>
Average	4.63 * 10 <sup>9</sup> c	7.8 * 10 <sup>9</sup> b	3.2 * 10 <sup>7</sup> a		
SD	1.4 * 10 <sup>9</sup>	7.7 * 10 <sup>9</sup>	4.0 * 10 <sup>7</sup>		

It is clear from Table (5) that the effect of voltage, type of bacteria, and the interaction between them is statistically significant (P< 0.05). Figure 11 shows the statistical variation of both types of bacteria when treated with jet plasma at different voltages. The plasma jet device is utilized to eradicate *E. coli* and *S. aureus* through the kill bacteria groups. An experiment to determine the colony-forming units (CFUs) was conducted immediately following the plasma treatment. Raising the plasma voltage applied to bacteria results in an augmentation of charge accumulation, hence intensifying the bacteria's rate of eradication. It is evident that the duration of exposure significantly impacts the killing rate, resulting in a decrease from 5×10<sup>9</sup> CFU per mL to a low value in the groups. Given that all bacterial samples in this study were subjected to indirect exposure to the plasma column[28].

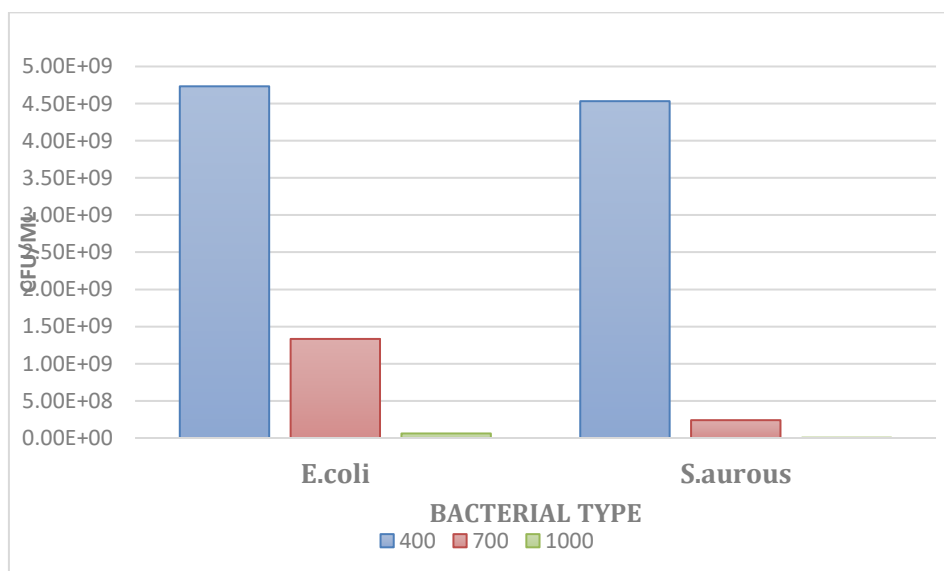


**Figure 11:** The statistical variation of *E. coli* and *S. aureus* through the utilization of a plasma jet apparatus.

**4-Conclusions**

The environment exerts a significant influence on the line intensity of the emission spectra produced by the plasma jet in cold plasma. The statistics revealed that the entry of argon gas has led to a rise in emission intensity, suggesting a higher concentration of gas molecules. Consequently, the common gas molecules passing through the plasma tube become ionized due to the electrolyte field's energy being adequate to induce secondary ionization of the molecules. The ionization of the moving gas converts into plasma at a rate of 4 liters per minute as the voltage fluctuates. As the gas current rate increases, the Debye duration, plasma frequency, and number of molecules on the surface all also rise. Additionally, the mortality of both bacterial populations was significantly impacted by voltage manipulation. This is due to the increased mortality rate caused by gas molecules adhering to the cellular structure. When the voltage hit its peak of 1000 volts, the groups' influence became clear. The killing of

bacteria using plasma jets is facilitated by the generation of reactive species that cause cellular damage, their non-thermal nature that allows safe application on tissues, and their effectiveness against antibiotic-resistant strains and biofilms.

### Conflict of interest

The authors declare that they have no conflicts of interest.

### References

- [1] G. Busco, E. Robert, N.Chettouh-Hammas, J.M. Pouvesle, and C. Grillon, "The emerging potential of cold atmospheric plasma in skin biology," *Free Radical Biology and Medicine*, Vol.161, pp.290-304.2020. doi.org/10.1016/j.freeradbiomed.2020.10.004.
- [2] S. Mošovská, V. Medvecká, L. Valík, A. Mikulajová, and A. Zahoranová, "Modelling of inactivation kinetics of Escherichia coli, Salmonella Enteritidis and Bacillus subtilis treated with a multi-hollow surface dielectric barrier discharge plasma," *Scientific Reports*, Vol.13 ,no.1, p.12058. 2023, https://doi.org/10.1038/s41598-023-38892-2.
- [3] R. Wang, , Y. Yang, S. Chen, H. Jiang, and P. Martin," Power calculation of pulse power-driven DBD plasma," *IEEE Transactions on Plasma Science*, Vol.49, no. 7, pp.2210-2216. 2021, DOI: 10.1109/TPS.2021.3084601.
- [4] B. Boekema, M Stoop, M. Vlig, J.van Liempt, A. Sobota, , M. Ulrich, and E. Middelkoop, "Antibacterial and safety tests of a flexible cold atmospheric plasma device for the stimulation of wound healing," *Applied Microbiology and Biotechnology*, Vol.105, pp.2057-2070. 2021, doi: 10.1007/s00253-021-11166-5
- [5] H.B. Baniya, R.P. Guragain, G.P. Panta, G. Qin, and D.P. Subedi, "Diagnostics of cold atmospheric pressure plasma jet and its antimicrobial properties," *AIP Conference Proceedings*. Vol. 2319, No. 1. 2021, doi.org/10.1063/5.0037121
- [6] A.I. Saifutdinov, B.A. Timerkaev, and A.A. Saifutdinov, " Features of transient processes in DC microdischarges in molecular gases: From a glow discharge to an arc discharge with a unfree or free cathode regime," *JETP Letters*, vol.112, pp.405-412. 2020, doi: 10.1134/S0021364020190091.
- [7] M. Javid, A. Haleem, R.P. Singh, and R. Suman, "Sustaining the healthcare systems through the conceptual of biomedical engineering: A study with recent and future potentials," *Biomedical Technology*, vol.1, pp.39-47. 2023. https://doi.org/10.1016/j.bmt.2022.11.004
- [8] X. Lu, D. Liu, Y. Xian, L. Nie , Y. Cao, and G. He , "Cold atmospheric-pressure air plasma jet: Physics and opportunities," *Physics of Plasmas*, Vol.28, no. 10 , 2021 , https://doi.org/10.1063/5.0067478.
- [9] B. B. Baldanov, "Experimental study of a multipoint cathode corona in an argon flow," *Plasma physics reports*. 2009 ;35:552-8., doi: 10.1134/s1063780x09070034.
- [10] T. von Woedtke, S. Emmert, H.R. Metelmann, S. Rumpf, and K.D. Weltmann," Perspectives on cold atmospheric plasma (CAP) applications in medicine," *Physics of Plasmas*, Vol.27, no.7 , 2020. doi: 27/7/070601/263334.
- [11] K.D. Weltmann, J. Winter, M. Polak, J. Ehlbeck, and von Woedtke, "Atmospheric pressure plasmas for decontamination of complex medical devices," *Medicine and Food Security* , vol.1 ,pp. 3-15, 2012. doi: 10.1007/978-94-007-2852-3\_1.
- [12] S. Siadati, M. Pet'ková, A.J. Kenari, S. Kyzek, E. Gálová, and A. Zahoranová, "Effect of a non-thermal atmospheric pressure plasma jet on four different yeasts," *Journal of physics D: Applied physics*, vol.54, no. 2, p.025204. 2020, doi: 10.1088/1361-6463/abb624.
- [13] E.M. Konchekov, V.V. Gudkova, D.E. Burmistrov, A.S. Konkova, M.A. Zimina, M.D. Khatueva, V.A. Polyakova, , A.A. Stepanenko, T.I.Pavlik, V.D. Borzosekov, and D.V.Malakhov, "Bacterial Decontamination of Water-Containing Objects Using Piezoelectric Direct Discharge Plasma and Plasma Jet," *Biomolecules*, vol.14 , no.2, p.181. 2024, doi.org/10.3390/biom14020181.
- [14] L. Pasquina-Lemonche, J. Burns, R.D. Turner, S. Kumar, R. Tank, N. Mullin, J.S. Wilson, B. Chakrabarti, , P.A. Bullough, S.J. Foster, and J.K. Hobbs, " The architecture of the Gram-positive bacterial cell wall," *Nature*, vol.582, no. 7811, pp.294-297, 2020. doi: s41586-020-2236-6 .

- [15] G.H. Jihad, M.A. Al-Sammarraie, and F. Al-Aani, "Effect of cold plasma technique on the quality of stored fruits-A case study on apples," *Revista Brasileira de Engenharia Agrícola e Ambiental*. Vol.19 , no.3 , pp.e276666, 2024, doi: 10.1590/1807-1929/agriambi.v28n3e276666.
- [16] D. K. Naser , A. K. Abbas and K. A. Aadim, "Zeta Potential of Ag, Cu, ZnO, CdO and Sn Nanoparticles Prepared by Pulse Laser Ablation in Liquid Environment," *Iraqi Journal of Science*, 2020, Vol. 61, No. 10, pp: 2570-2581.
- [17] K.A. Aadim, A.Z. Mohammad, and M.A. Abduljabbar, "Influence of laser energy on synthesizes of CdO/Nps in liquid environment," *IOP Conference Series: Materials Science and Engineering* ,Vol. 454, No. 1, p. 012028. 2018. doi: 10.1088/1757-899X/454/1/012028.
- [18] L. Zhang, D. Zhang, Y. Guo, Q. Zhou, H. Luo, and J. Tie, " Surface decontamination by atmospheric pressure plasma jet: Key biological processes," *Journal of Physics D: Applied Physics*, Vol.55, no.42, p.425203. 2022, doi: 10.1088/1361-6463/ac8432.
- [19] Z. M. Romi and M. E. Ahmed , "The Influence of Biologically Synthesized Copper Nanoparticles on the Biofilm Produced by Staphylococcus haemolyticus Isolated from Seminal Fluid ," *Iraqi Journal of Science*, Vol. 65, No. 4, 2024, pp: 1948-1968. DOI: 10.24996/ijs.2024.65.4.15.
- [20] X. Zhang, K.J. Liew, C.S. Chong, X. Cai, Z. Chang, H. Jia, P. Liu, H. He, W. Liu, and Y. Li, "Low-Temperature Air Plasma Jet for Inactivation of Bacteria (*S. aureus* and *E. coli*) and Fungi (*C. albicans* and *T. rubrum*)," *Acta Physica Polonica A* . vol.1 , pp.1898-794X. 2023, doi: 10.12693/APhysPolA.143.12.
- [21] K. Lotfy, "The impact of the carrier gas composition of non-thermal atmospheric pressure plasma jet for bacteria sterilization," *AIP Advances*, vol.10 , no.1,pp.1-10 , 2020, doi: 10.1063/1.5099923.
- [22] H.E. Bousba, S. Sahli, W. Seif, E. Namous, L. Benterrouche, and M. Saoudi, " Inactivation of Escherichia coli in water using cold atmospheric plasma jet," *In 2022 2nd International Conference on Advanced Electrical Engineering (ICAEE)* ,pp. 1-4, 2022., doi: 10.1109/ICAEE53772.2022.9962110
- [23] H. Suzuki, T. Ogasawara, Y. Iwata, H. Bae, and H. Toyoda, " High-speed hydrophilic and ashing treatments of polyimide using Ar/O<sub>2</sub> atmospheric-pressure microwave line plasma," *Japanese Journal of Applied Physics*, Vol. 61, p.S11008. 2022 , doi: 10.35848/1347-4065/ac64e2.
- [24] K. Shang, J. Li, X. Wang, D. Yao, N. Lu, Jiang, and Y. Wu, "Evaluating the generation efficiency of hydrogen peroxide in water by pulsed discharge over water surface and underwater bubbling pulsed discharge," *Japanese Journal of Applied Physics*. Vol.29 , no.1 , pp. 01AB02 , 2015 , doi: 10.7567/JJAP.55.01AB02.
- [25] Y. Chen, W. Chung, B. Tong, and M.B. Chang, "Evaluation of the effectiveness of nonthermal plasma disinfection," *Environmental technology*. Vol.41 , no.21 ,2020 , doi: 10.1080/09593330.2019.1583289.
- [26] A. Sakudo, Y. Yagyū, and T. Onodera. "Disinfection and sterilization using plasma technology: Fundamentals and future perspectives for biological applications," *International journal of molecular sciences*, Vol.20, no.20, p.5216. 2019 , doi: 1422-0067/20/20/5216
- [27] T.F. Orabi , and K.A. Aadim, "Spectroscopic diagnosis of nickel and zinc plasmas produced by plasma jet technique," *Journal of Optics*, Vol.5 pp.1-7. 2024 , doi: 10.1007/s12596-024-01891-1.
- [28] M. M. Hameed , Abdul-Majeed E. Al-Samarai and K. A. Aadim, "Synthesis and Characterization of Gallium Oxide Nanoparticles using Pulsed Laser Deposition," *Iraqi Journal of Science*, vol. 61, no. 10, pp. 2582-2589, 2020.